Improved order and transport in C60 thin films grown on SiO2 via use of transient templates

Jakub Hagara, Hongwon Kim, Jan Hagenlocher, Ivan Zaluzhnyy, Alexander Gerlach, Alexander Hinderhofer, Stephan V. Roth, Wolfgang Brütting, Frank Schreiber

Angaben zur Veröffentlichung / Publication details:

Hagara, Jakub, Hongwon Kim, Jan Hagenlocher, Ivan Zaluzhnyy, Alexander Gerlach, Alexander Hinderhofer, Stephan V. Roth, Wolfgang Brütting, and Frank Schreiber. 2022. "Improved order and transport in C60 thin films grown on SiO2 via use of transient templates." *Applied Physics Letters* 121 (18): 182101. https://doi.org/10.1063/5.0102508.

Applied Physics Letters ARTICLE scitation.org/journal/apl

Improved order and transport in C_{60} thin films grown on SiO_2 via use of transient templates

Cite as: Appl. Phys. Lett. **121**, 182101 (2022); doi: 10.1063/5.0102508
Submitted: 10 June 2022 · Accepted: 5 October 2022 ·
Published Online: 1 November 2022

Jakub Hagara,[1,a)] Hongwon Kim,[2] Jan Hagenlocher,[1] Ivan Zaluzhnyy,[1] Alexander Gerlach,[1] Alexander Hinderhofer,[1] Stephan V. Roth,[3] Wolfgang Brütting,[2] and Frank Schreiber[1]

AFFILIATIONS

[1]Institute of Applied Physics, University of Tübingen, Auf der Morgenstelle 10, 72076 Tübingen, Germany
[2]Institute of Physics, University of Augsburg, Universitätsstraße 1, 86159 Augsburg, Germany
[3]Deutsches Elektronen-Synchrotron (DESY), Notkestraße 85, 22607 Hamburg, Germany

[a)]Author to whom correspondence should be addressed: jakub.hagara@uni-tuebingen.de

ABSTRACT

The performance of C_{60} semiconducting films is linked to the degree of crystallinity and ordering, properties that strongly depend on the substrate, and growth conditions. Substrate–molecule interactions can be specifically tailored by employing growth templates to achieve a desired thin film structure. However, the presence of a growth template after the film deposition is usually not desirable as it may change the properties of the layer of interest. The ability to remove a growth template without any disruption to the active layer would be highly beneficial. A simple method of template removal by annealing is presented here. A variety of small organic molecules (perfluoropentacene, [6]phenacene, and α-sexithiophene) were used as a growth template to obtain a high-quality well-ordered C_{60} thin film. *In situ* grazing-incidence wide-angle x-ray scattering was employed to study the structural changes of C_{60} thin films during template removal. While a slight disturbance of the thin film structure was observed during template removal caused by evaporated molecules from the growth template escaping through the C_{60} layer, the disruption is only temporary. When the annealing process is concluded, only the well-ordered C_{60} thin film directly on top of SiO_2 is left, which is not achievable without the use of a growth template. Improved crystallinity and grain size of such a thin film, when compared to preparation without a growth template, lead to a significant improvement of the charge carrier mobility. Importantly, template removal prevents the formation of undesired ambipolar transistor characteristics.

The controlled growth of organic thin films, used as active layers in many device applications, is a serious challenge particularly for the deposition of molecular semiconductors.[1–3] On a fundamental level, the growth behavior of thin films is determined by a complex interplay of a number of energetic and kinetic factors. For each given system, a suitable window of parameters including temperature and deposition rate has to be identified individually, and it is by no means clear that there is a process window leading to smooth layer-by-layer growth on a given substrate.[4] An anisotropic shape of most organic molecules introduces further challenges related to their orientational degrees of freedom, since the orientation of a given molecule is an additional source of disorder compared to elemental systems.[5–7] Essentially, the only exception in this context is C_{60}, since at room temperature, its net interaction potential averages to an effectively spherical one,[8–10] but it should be noted that the interaction is short-ranged compared to atoms, causing differences in the resulting growth behavior.[11] C_{60} and its derivatives also play a rather special role in the context of spectroscopic and functional properties, including applications in organic photovoltaics (OPVs).[12,13] This makes it particularly important to understand its growth behavior. In practice, the growth of well-defined C_{60} thin films has proven to be nontrivial.[8,14,15]

One way of attempting to modify the growth is by changing the substrate. For instance, a stepped substrate can induce better lateral order and/or azimuthal orientation of the crystallites.[16,17] Varying the chemical nature of the substrate, thus the molecule–substrate interaction, can induce entirely different phases or orientations of the growing film.[6] However, for specific device applications, technical reasons often confine the choice of substrate. In such cases, interface energy and, consequently, the growth may still be modified using templating layers (TLs), as it was demonstrated that different organic surfaces induce an entirely different growth behavior of C_{60}.[15,18,19]

Organic growth templates have shown to be an enticing tool to aid the preparation of high-quality thin films used in organic semiconducting devices.[20–23] Growth templates are mainly used to promote high crystallinity and specific molecular ordering, which attribute particularly important for high-performance organic

TABLE I. Charge transport parameters for C_{60} films without and with templating.

	V_T (V)	μ_e ($cm^2 V^{□1} s^{□1}$)	I_{ON}/I_{OFF}
C_{60}	61.2	8.2 □ $10^{□3}$	10^4–10^5
Templated C_{60}	56.8	2.9 □ $10^{□1}$	10^6

field-effect transistors (OFETs) and organic photovoltaics (OPVs), where the charge-carrier mobility is greatly influenced by the molecular packing.[24–27] In that context, suitable growth templates that lead to improved (opto)electronic properties of the organic semiconducting layers are highly desirable. Organic molecules used in this work as growth templates have a rod-like shape, where one dimension of the molecules is significantly longer than the rest. This type of molecules is known to grow with a standing-up orientation on amorphous substrates such as SiO_2.[28,29] As demonstrated before, C_{60} molecules deposited on top of template layers with such a molecular orientation grow with improved ordering and larger grain sizes,[18,30–33] which translates to improved semiconducting properties of the organic thin film.[18]

The presence of a growth template after the thin film preparation is, however, not required for a proper function of an active layer. In some cases, it might even actively hinder the performance of the produced device. Most commonly used growth templates display a strong anisotropy of their physical properties, namely, charge-carrier mobility. The in-plane mobility of two-dimensional (2D) growth templates such as MoS_2, $MoSe_2$, GaN, and graphene is several orders of magnitude higher than in a direction perpendicular to individual layers.[34,35] Similarly, growth templates based on small organic molecules exhibit substantially higher charge-carrier mobility in the π–π stacking direction of their conjugated cores.[36] For both types of templates, the in-plane mobility would dominate the charge transport. The presence of such a growth template underneath an active layer would be detrimental to the performance of vertical OFETs, where an active layer is sandwiched between source and drain electrodes.[37] Additionally, due to relatively high charge-carrier mobility of most commonly used organic growth templates, depending on the character of both materials, the presence of a templating layer can lead to undesirable ambipolar behavior of the organic semiconducting thin film, which is unfavorable in terms of their potential use in logic electronic circuits.[18,20] The ability to remove a growth template after an active layer preparation while retaining a well-ordered thin film structure would be highly beneficial.

In this work, we deposited a C_{60} thin film on a variety of organic growth templates (Fig. 1): perfluoropentacene (PFP), [6]phenacene (6Phe), and α-sexithiophene (α-6T). These growth templates promote the formation of well-defined highly crystalline C_{60} thin films that are suitable for use in organic electronic devices. We observe the nucleation of an oriented and well-ordered C_{60} thin film structure, in contrast to amorphous films commonly obtained when depositing C_{60} directly onto a silicon substrate. However, the presence of a growth template after the deposition might not be desired for the use of C_{60} thin films in specific applications. We present a simple method of template removal by sample annealing. We show that this process leads to the removal of the organic growth template layer and leaves an intact C_{60} thin film that retains its highly crystalline structure. Employing grazing-incidence wide-angle x-ray scattering (GIWAXS) measurements, we study the process of template evaporation and any structural changes of the prepared thin film that might occur as a result of sample annealing. The impact of the template removal on the topography of a C_{60} thin film is further investigated by AFM imaging.

Organic growth templates in a form of 20 nm thin layer were deposited onto a silicon substrate using organic molecular beam deposition (OMBD) at substrate temperature T¼ 300 K in an ultra-high vacuum (UHV) growth chamber. C_{60} thin films with the effective thickness of 25 nm were then deposited directly on top of an organic growth template by OMBD at the same growth conditions. *In situ* grazing-incidence wide-angle x-ray scattering (GIWAXS) measurements of C_{60} thin films on various organic growth templates during the template removal were performed at DESY (Hamburg, Germany) on beamline P03. During the measurements, the samples were located

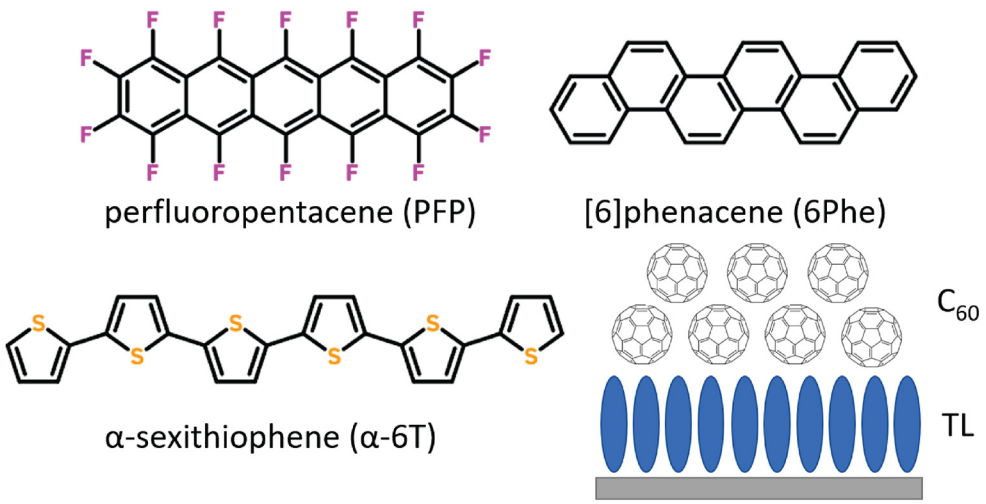

FIG. 1. Structural formula of perfluoropentacene, [6]phenacene, and α-sexithiophene used for the templating layer (TL) and schematic illustration of a TL with standing-up configuration.

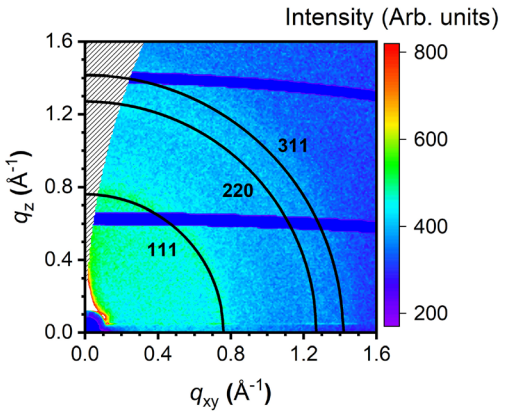

FIG. 2. GIWAXS pattern of polycrystalline C_{60} on a SiO_2 substrate.

inside a small vacuum chamber equipped with a graphite dome for the x-ray beam to pass through. During the *in situ* measurements, the samples were gradually heated up at a rate of 12 °C/min in order to evaporate the organic template layer. Atomic force microscopy (AFM) was then employed to study the topography of the prepared thin films using a JPK NanoWizard II (Bruker, USA) in intermittent contact (air) mode. To investigate the impact of the growth template on the charge-carrier mobility of C_{60} thin films, OFET devices were fabricated in the top-contact/bottom-gate geometry on p-doped Si/SiO_2 wafers [$Si^{þ þ}/SiO_2$(300 nm)/C_{60}/Al]. The mobility measurements were performed in vacuum (>10^{-7} mbar) using a parameter analyzer (Keithley 4200A-SCS, USA). More information about OFET device fabrication and geometry can be found in the supplementary material.

We studied the crystallinity and thin film structure of C_{60} on various molecular templates by GIWAXS. All compounds used as growth templates were selected due to their ability to create oriented and highly crystalline thin film structures.[38–40]

C_{60} thin films deposited directly onto the amorphous substrates such as SiO_2 have a polycrystalline structure without preferential orientation as evidenced by the presence of isotropic Debye–Scherrer ring features (Fig. 2) rather than defined spots. When the same films are deposited on top of a substrate with a templating layer at the identical deposition conditions, growth behavior differs substantially. Reciprocal space maps in Fig. 3 show pronounced reflection spots arising from the ordered structure of C_{60} as well as from an organic template. The expected standing-up configuration of the organic growth templates is confirmed by the out-of-plane position of the 002 reflection partially hidden by the "missing wedge." This reflection in q_z direction of the reciprocal space map results from the ordered stacking of molecules in the direction perpendicular to the surface of the substrate with the *d*-spacing roughly corresponding to the length of the organic template molecule. Clearly visible reflections with non-zero *h* and *k* indices convey an exceptional ordering even in the in-plane direction. The C_{60} thin layer exhibits equally remarkable ordering both in the in-plane and out-of-plane directions as shown by the presence of numerous reflection spots marked in Fig. 3. All observed C_{60} reflections are well-defined, indicating that all grains of the thin film show the same orientation of lattice planes relative to the surface normal. From the position of the reflections in the reciprocal space maps, a full set of unit cell parameters as well as the orientation of crystallographic planes with respect to the sample surface can be determined. C_{60} molecules on the organic template layers assemble in a face-centered cubic (fcc) structure with the unit cell parameter a ¼ 14.296 Å and with the (111) lattice planes parallel to the substrate surface.[41] The fact that exactly the same structure is observed on all molecular templates (see Fig. S2 in the supplementary material) shows that the thin film structure of C_{60} does not depend on the type of organic molecule used for the templating layer. The same well-ordered thin film structure can also be observed when C_{60} is grown on inorganic two-dimensional substrates such as MoS_2, GaSe, or GeS.[42,43]

We can conclude that molecular templates have a significant impact on the growth of C_{60}, promoting the crystallization of well-ordered thin films. However, the presence of the underlying template layer is often undesirable as it might hamper the performance of the active layer. Removal of the growth template without disruption of crystallinity and structure of the desired layer would be needed. The high sublimation temperature of C_{60} compared to other commonly used organic materials allows the removal of the organic growth templates by thermal annealing. We used *in situ* real-time GIWAXS to monitor the structural changes during the process of template

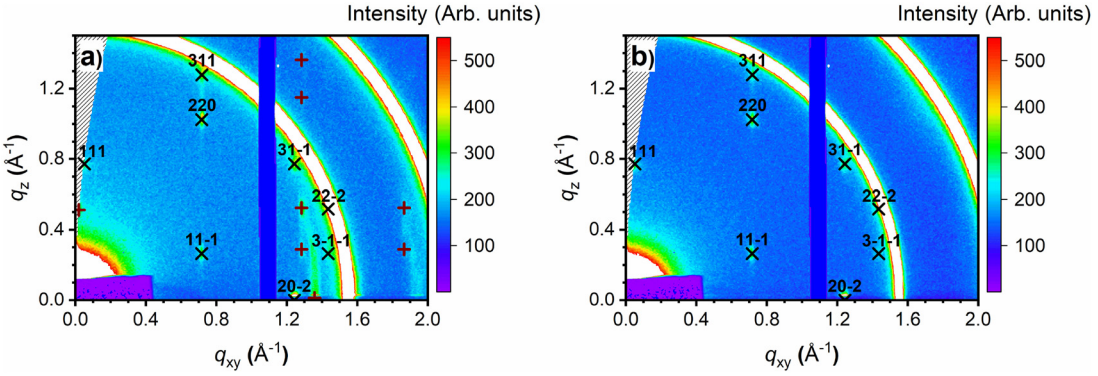

FIG. 3. GIWAXS pattern of 25 nm C_{60} thin films deposited on top of 20 nm α-6T growth template (a) before and (b) after the template removal process. Black "x" marks with Miller indices denote the Bragg reflections arising from the fcc structure of C_{60}, and brown "þ" marks indicate reflections from the α-6T templating layer. Ring features arise from the graphite dome used in the experimental setup.

removal. The intensity of the Bragg reflections was tracked for both the C_{60} thin film and the organic templates. The sample holder was gradually heated up with a temperature increase of 12 °C per minute up to 250 °C to remove the organic growth template. It is important to note that desorption of C_{60} molecules starts well above the temperature used for the template removal. Figure 4(a) shows the evolution of peak intensities with increasing substrate temperature. When the temperature of the sample starts reaching the sublimation temperature of the organic growth template, there is a gradual decrease in peak intensity for peaks belonging to the template. This can be attributed to both the decrease in crystallinity and the loss of material as molecules of an underlying growth template are slowly evaporating from the sample. The C_{60} layer on top of an organic growth template forms a homogeneous and continuous layer as shown in Fig. 4(c). Evaporated molecules of the template layer need to escape through the C_{60} thin film, disrupting its structure as evidenced by a slight intensity decrease in the C_{60} peaks. After the template layer is fully evaporated, indicated by the complete disappearance of the corresponding Bragg peaks, the ordering of the C_{60} thin film is restored as shown by peak intensity returning to previous values. Interestingly, there is an observable increase in the 002 intensity from C_{60} after the full evaporation of the growth template. As no new material is deposited during the template removal, this intensity increase can be attributed solely to an improved out-of-plane ordering. A possible explanation would be that the C_{60} thin film now lies directly on top of a SiO_2 substrate that is much smoother compared to the relatively rough surface of an organic growth template.

By tracking the positions of Bragg peaks during the template removal, we observed only a slight temporary disturbance in C_{60} thin film structure (see Fig. S3 in the supplementary material), which does not lead to measurable change of unit cell parameters at any point during the annealing process. The GIWAXS patterns before and after template removal (Fig. 3) then show that the C_{60} thin film structure is preserved without any measurable degradation or change in orientation of C_{60} domains.

Additionally, AFM was employed to study the topography of a C_{60} thin film before and after the template evaporation. Figure 4 shows differences between C_{60} thin films (b) deposited directly onto a SiO_2 substrate, (c) deposited onto a templating layer, and (d) after the template removal. The estimated average C_{60} grain size for thin films deposited directly on silicon substrates based on AFM images is 15 nm. Employing a templating layer, the average grain size is increased to an average of 89 nm before and 86 nm after template removal. As will be demonstrated below, larger average grain sizes,

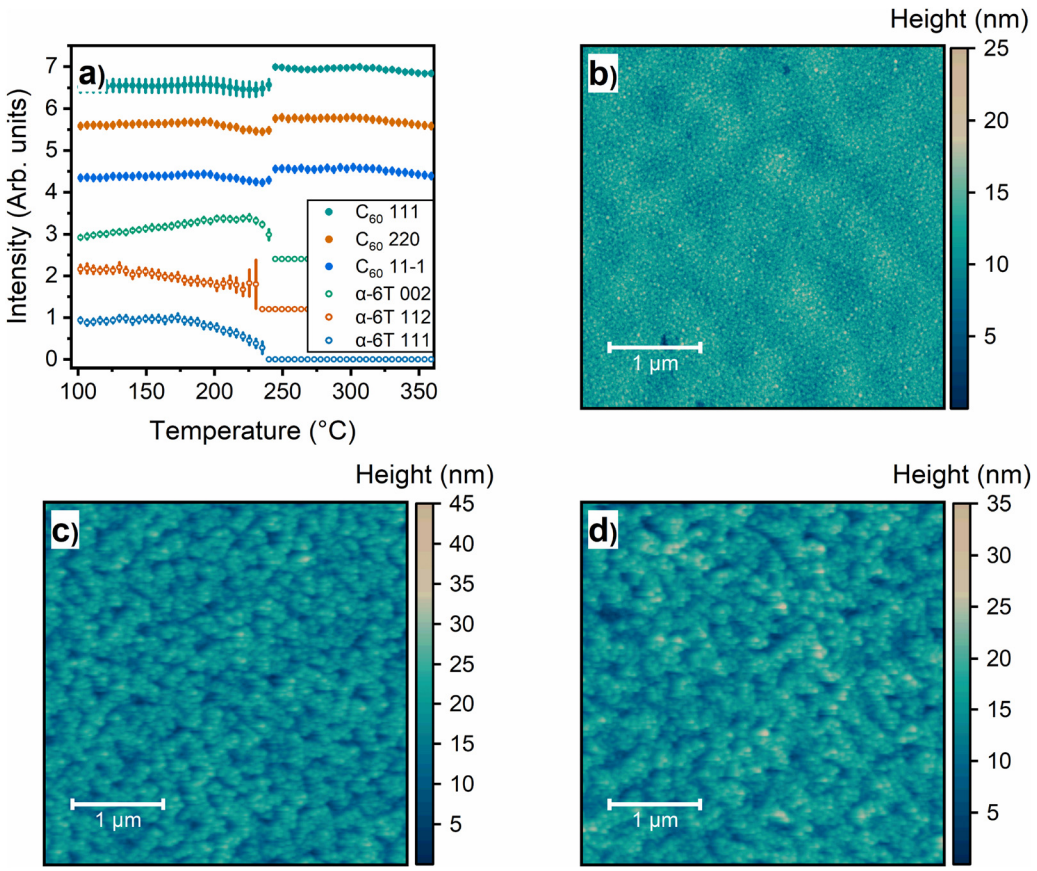

FIG. 4. (a) Evolution of peak intensities for selected peaks of C_{60} and α-6T during the template removal. (b) AFM image of C_{60} on SiO_2, (c) AFM image of C_{60} on growth template, and (d) AFM image of C_{60} after the template removal.

and therefore a decreased number of grain boundaries, yield a significant improvement of the electronic properties of the C_{60} film. Another relevant aspect is the investigation of possible changes in the morphology of the C_{60} thin films after the template removal. The homogeneity of the C_{60} layer as well as the presence of narrow gaps after the template removal process depends on how fast the templating molecules are desorbed. At lower desorption rates, when the substrate is heated up at low rate (□5 □C/min), the template removal process has no significant impact on the C_{60} film as AFM images of the C_{60} sample before [Fig. 4(c)] and after the template removal [Fig. 4(d)] are almost identical [as shown by power spectral density function (PSDF) extracted from AFM images (Fig. S6 in the supplementary material)]. The C_{60} layer after template removal appears homogeneous and intact without visible gaps or cracks that might be expected due to layer disruption by escaping template molecules. Only when the desorption rate is high enough, caused by fast substrate heating rate during the template removal (15 □C/min), homogeneity of the final C_{60} layer is permanently altered by the presence of narrow trenches caused by escaping template molecules (Fig. S4 in the supplementary material).

Electrical characteristics of C_{60} OFETs without and with templating by α-6T are shown in Fig. 5 and in Table I. They show n-type behavior with electron transfer at positive gate-source biases. The threshold voltage V_T for both devices is comparable at 61.2 V for non-templated and 56.8 V for templated C_{60} device. The charge-carrier mobility for electrons μ_e in the linear region ($V_D < V_G - V_T$) was calculated using the following equation:

$$I_{D,lin} = \frac{W}{L}\mu_e C_i(V_G - V_T)V_D,$$

where I_D is the source–drain current, V_D is the applied source–drain voltage, C_i is the gate insulator capacitance per unit area, and W and L are the width and length of the transistor channel, respectively. A linear fit was applied to the I_D vs V_D data in order to derive the electron mobility μ_e. The threshold voltages were calculated as the x-intersect of $I_D^{1/2}$ vs V_G curve in the saturation regime ($V_D > V_G - V_T$) using the following equation:

$$I_{D,sat} = \frac{W}{2L}\mu_e C_i(V_G - V_T)^2.$$

A mobility of 8.2 □ $10^{□3}$ $cm^2/V\,s$ was measured for non-templated C_{60}, while for templated C_{60} thin film, a value of 2.9 □ $10^{□1}$ $cm^2/V\,s$ was obtained. This substantial improvement in electron mobility is attributed to enhanced ordering of C_{60} layer promoted by a templating layer. To demonstrate the crucial benefit of the template removal process, we also compared OFET characteristics of templated C_{60} devices before and after template removal (Fig. S8 in the supplementary material). Both devices show improved electron mobility when compared to the C_{60} device prepared without the templating layer. However, when the templating layer is still present, OFET devices show ambipolar behavior due to relatively high hole mobility of the used templating layer. Ambipolar behavior is not desirable for most device applications. After the template removal, the hole transport channel is lost while the improved electron mobility is retained.

To conclude, we have grown C_{60} thin films on top of various organic template layers and studied their effect on the structure of the deposited thin film. We observe that when a templating layer is used, C_{60} forms an oriented and well-ordered thin film as opposed to randomly oriented grains commonly observed when deposited straight onto a silicon substrate. While the highly crystalline C_{60} thin film is attractive for use in organic electronic devices, the presence of an underlying organic template might be undesirable for specific applications. We used a simple process of annealing to remove the organic growth template. We studied the processes and structural changes of the investigated thin films during the template removal employing *in situ* real-time GIWAXS. When the sublimation temperature is reached during the template removal, molecules of the template layer are escaping through the C_{60} thin film. Remarkably, after the evaporation of the templating layer, the ordering of the C_{60} layer is restored to the state before annealing. Template removal also does not affect the thin film structure as unit cell parameters remain constant during the whole process. The C_{60} thin film integrity without gaps or cracks is further confirmed by AFM. The improved ordering of the C_{60} layer proved to be beneficial for the OFET characteristics of the corresponding films. Furthermore, the removal of the templating layer prevents the OFETs from becoming ambipolar. Generally, transient templates might be an important step for organic layers with respect to their use in practical applications.

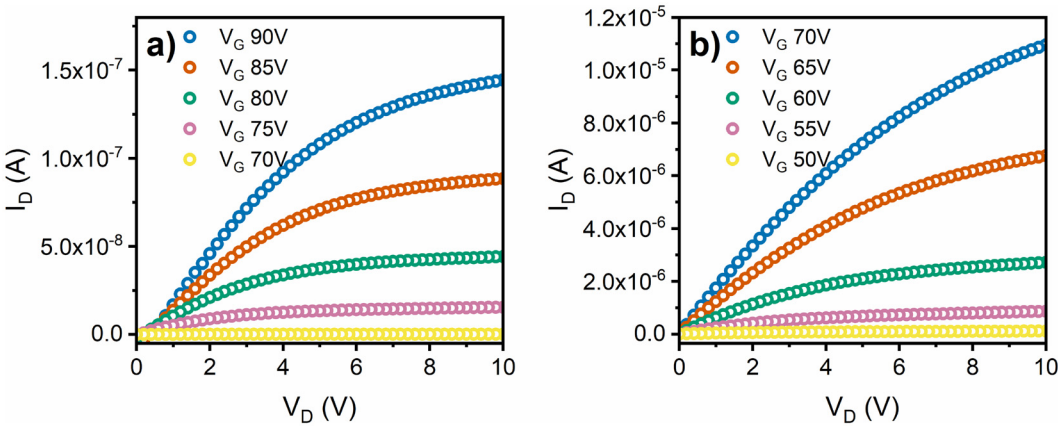

FIG. 5. OFET characteristics for C_{60} (a) without templating (b) using α-6T growth template after template removal.

See the supplementary material for GIWAXS patterns of all used templating layers before and after the template removal, C_{60} peak position evolution evaluated from *in situ* GIWAXS measurements during the template removal process, PSDF extracted from AFM images, and OFET device preparation and geometry description.

The authors gratefully acknowledge the financial support of the German Research Foundation (Deutsche Forschungsgemeinschaft, DFG), Projects SCHR 700/20-2 & BR 1728/14-2 (Project No. 239543752), and Carl Zeiss Foundation. We would also like to thank the Deutsches Elektronen-Synchrotron (DESY) for providing the exceptional facilities at the P03 beamline.

AUTHOR DECLARATIONS

Conflict of Interest

The authors have no conflicts to disclose.

Author Contributions

Jakub Hagara: Conceptualization (equal); Data curation (equal); Formal analysis (equal); Investigation (equal); Methodology (equal); Visualization (equal); Writing – original draft (equal). **Hongwon Kim:** Data curation (equal); Formal analysis (equal); Investigation (equal); Visualization (equal); Writing – original draft (equal). **Jan Hagenlocher:** Investigation (equal). **Ivan A. Zaluzhnyy:** Investigation (equal); Writing – review & editing (equal). **Alexander Gerlach:** Conceptualization (equal); Project administration (equal); Supervision (equal); Writing – review & editing (equal). **Alexander Hinderhofer:** Conceptualization (equal); Investigation (equal); Project administration (equal); Supervision (equal); Writing – review & editing (equal). **Stephan Volkher Roth:** Methodology (equal); Resources (equal); Writing – review & editing (equal). **Wolfgang Brütting:** Conceptualization (equal); Formal analysis (equal); Funding acquisition (equal); Methodology (equal); Resources (equal); Supervision (equal); Writing – review & editing (equal). **Frank Schreiber:** Conceptualization (equal); Funding acquisition (lead); Project administration (equal); Resources (equal); Supervision (equal); Writing – review & editing (equal).

DATA AVAILABILITY

The data that support the findings of this study are available from the corresponding author upon reasonable request.

REFERENCES

[1]G. Witte and C. Wöll, J. Mater. Res. **19**, 1889 (2004).
[2]F. Schreiber, Phys. Status Solidi A **201**, 1037 (2004).
[3]A. Winkler, Surf. Sci. **643**, 124 (2016).
[4]T. Michely and J. Krug, *Islands, Mounds and Atoms* (Springer, Berlin, Heidelberg, 2012).
[5]R. Ruiz, D. Choudhary, B. Nickel, T. Toccoli, K.-C. Chang, A. C. Mayer, P. Clancy, J. M. Blakely, R. L. Headrick, S. Iannotta, and G. G. Malliaras, Chem. Mater. **16**, 4497 (2004).
[6]S. Kowarik, A. Gerlach, S. Sellner, F. Schreiber, L. Cavalcanti, and O. Konovalov, Phys. Rev. Lett. **96**, 125504 (2006).
[7]A. C. Dürr, F. Schreiber, K. A. Ritley, V. Kruppa, J. Krug, H. Dosch, and B. Struth, Phys. Rev. Lett. **90**, 016104 (2003).
[8]S. Bommel, N. Kleppmann, C. Weber, H. Spranger, P. Schäfer, J. Novak, S. V. Roth, F. Schreiber, S. H. L. Klapp, and S. Kowarik, Nat. Commun. **5**, 5388 (2014).
[9]W. Janke and T. Speck, J. Chem. Phys. **154**, 234701 (2021).
[10]W. Janke and T. Speck, Phys. Rev. B **101**, 125427 (2020).
[11]N. Kleppmann, F. Schreiber, and S. H. L. Klapp, Phys. Rev. E **95**, 20801 (2017).
[12]W. Brütting, *Physics of Organic Semiconductors* (Wiley-VCH Weinheim, 2005).
[13]J. Wagner, M. Gruber, A. Hinderhofer, A. Wilke, B. Bröker, J. Frisch, P. Amsalem, A. Vollmer, A. Opitz, N. Koch, F. Schreiber, and W. Brütting, Adv. Funct. Mater. **20**, 4295 (2010).
[14]R. L. Headrick, J. G. Ulbrandt, P. Myint, J. Wan, Y. Li, A. Fluerasu, Y. Zhang, L. Wiegart, and K. F. Ludwig, Nat. Commun. **10**, 2638 (2019).
[15]A. Huttner, T. Breuer, and G. Witte, ACS Appl. Mater. Interfaces **11**, 35177 (2019).
[16]J. O. Ossó, F. Schreiber, V. Kruppa, H. Dosch, M. Garriga, M. I. Alonso, and F. Cerdeira, Adv. Funct. Mater. **12**, 455 (2002).
[17]T. Breuer and G. Witte, ACS Appl. Mater. Interfaces **5**, 9740 (2013).
[18]K. Itaka, M. Yamashiro, J. Yamaguchi, M. Haemori, S. Yaginuma, Y. Matsumoto, M. Kondo, and H. Koinuma, Adv. Mater. **18**, 1713 (2006).
[19]I. Salzmann, S. Duhm, R. Opitz, R. L. Johnson, J. P. Rabe, and N. Koch, J. Appl. Phys. **104**, 114518 (2008).
[20]L. Huang, F. Zhu, C. Liu, H. Wang, Y. Geng, and D. Yan, Org. Electron. **11**, 195 (2010).
[21]F. Pan, H. Tian, X. Qian, L. Huang, Y. Geng, and D. Yan, Org. Electron. **12**, 1358 (2011).
[22]W. Zhao, J. P. Mudrick, Y. Zheng, W. T. Hammond, Y. Yang, and J. Xue, Org. Electron. **13**, 129 (2012).
[23]J. Guo, D. Liu, W. Li, B. Yu, H. Tian, F. Zhu, and D. Yan, Org. Electron. **93**, 106170 (2021).
[24]Y. Yuan, G. Giri, A. L. Ayzner, A. P. Zoombelt, S. C. B. Mannsfeld, J. Chen, D. Nordlund, M. F. Toney, J. Huang, and Z. Bao, Nat. Commun. **5**, 3005 (2014).
[25]M. Mas-Torrent and C. Rovira, Chem. Rev. **111**, 4833 (2011).
[26]S. H. Liu, W. M. Wang, A. L. Briseno, S. C. B. Mannsfeld, and Z. N. Bao, Adv. Mater. **21**, 1217 (2009).
[27]A. A. Virkar, S. Mannsfeld, Z. Bao, and N. Stingelin, Adv. Mater. **22**, 3857 (2010).
[28]J. Yang, D. Yan, and T. S. Jones, Chem. Rev. **115**, 5570 (2015).
[29]M. K. Huss-Hansen, M. Hodas, N. Mrkyvkova, J. Hagara, P. Nadazdy, M. Sojkova, S. O. Høegh, A. Vlad, P. Pandit, E. Majkova, P. Siffalovic, F. Schreiber, J. Kjelstrup-Hansen, and M. Knaapila, Phys. Rev. Mater. **5**, 053402 (2021).
[30]B. R. Conrad, J. Tosado, G. Dutton, D. B. Dougherty, W. Jin, T. Bonnen, A. Schuldenfrei, W. G. Cullen, E. D. Williams, J. E. Reutt-Robey, and S. W. Robey, Appl. Phys. Lett. **95**, 213302 (2009).
[31]A. Hinderhofer, A. Gerlach, K. Broch, T. Hosokai, K. Yonezawa, K. Kato, S. Kera, N. Ueno, and F. Schreiber, J. Phys. Chem. C **117**, 1053 (2013).
[32]Y.-T. Fu, C. Risko, and J.-L. Brédas, Adv. Mater. **25**, 878 (2013).
[33]Y. M. Acevedo, R. A. Cantrell, P. G. Berard, D. L. Koch, and P. Clancy, Langmuir **32**, 3045 (2016).
[34]M. D. Siao, W. C. Shen, R. S. Chen, Z. W. Chang, M. C. Shih, Y. P. Chiu, and C.-M. Cheng, Nat. Commun. **9**, 1442 (2018).
[35]K. S. Krishnan and N. Ganguli, Nature **144**, 667 (1939).
[36]J. R. Ostrick, A. Dodabalapur, L. Torsi, A. J. Lovinger, E. W. Kwock, T. M. Miller, M. Galvin, M. Berggren, and H. E. Katz, J. Appl. Phys. **81**, 6804 (1997).
[37]Y. Yang and A. J. Heeger, Nature **372**, 344 (1994).
[38]Y. Inoue, Y. Sakamoto, T. Suzuki, M. Kobayashi, Y. Gao, and S. Tokito, Jpn. J. Appl. Phys. **44**, 3663 (2005).
[39]G. Horowitz, F. Garnier, A. Yassar, R. Hajlaoui, and F. Kouki, Adv. Mater. **8**, 52 (1996).
[40]N. Komura, H. Goto, X. He, H. Mitamura, R. Eguchi, Y. Kaji, H. Okamoto, Y. Sugawara, S. Gohda, K. Sato, and Y. Kubozono, Appl. Phys. Lett. **101**, 083301 (2012).
[41]D. L. Dorset and M. P. McCourt, Acta Crystallogr. Sect. A **50**, 344 (1994).
[42]M. Sakurai, H. Tada, K. Saiki, and A. Koma, Jpn. J. Appl. Phys. **30**, L1892 (1991).
[43]G. Gensterblum, L. M. Yu, J. J. Pireaux, P. A. Thiry, R. Caudano, J. M. Themlin, S. Bouzidi, F. Coletti, and J. M. Debever, Appl. Phys. A **56**, 175 (1993).